

Water Adsorption on (111) Surfaces of BaF_2 and CaF_2

J. C. Zink, J. Reif, and E. Matthias

Institut für Experimentalphysik, Freie Universität Berlin, Arnimallee 14, W-1000 Berlin 33, Germany

(Received 2 March 1992)

Water adsorption on polished (111) surfaces of BaF_2 and CaF_2 was studied at room temperature under ultrahigh vacuum conditions by optical second-harmonic generation. Above 10^4 langmuirs, the total second-harmonic yield decreases with increasing exposure. The azimuthal anisotropy is influenced differently on each substrate. Below 10^4 langmuirs the $3m$ symmetry of the crystal surface is preserved in both cases, but more pronounced for CaF_2 . At high doses the symmetry remains for BaF_2 , but vanishes for CaF_2 . The results point to pseudomorphous epitaxial growth of water on BaF_2 but not on CaF_2 .

PACS numbers: 68.55.-a, 42.65.Ky, 68.35.Bs

The problem of molecular water adsorption on surfaces is of general interest, and considerable research effort has been devoted to this topic. A comprehensive review of the field, focusing on metal, semiconductor, and oxide substrates, is given in Ref. [1]. Much less is known about water growth on nonoxidic ionic surfaces. Early work [2-4] on polycrystalline alkali halides was mostly concerned with the adsorption site and the question of two-dimensional condensation or well-defined adsorbate layers. Secondary ion mass spectroscopy (SIMS) in ultrahigh vacuum (UHV) led to the result [5,6] that H_2O adsorbs on cleaved alkali halide surfaces only at low substrate temperatures (≤ 200 K). This work also called attention to the importance of "active sites" for adsorption, consisting of structural defects, color centers, or impurities in the surface layer, which may or may not be removable by heat treatment. For $\text{LiF}(001)$, e.g., heating of the surface to 700 K led to complete inertness against water up to a partial pressure of 10^{-7} Torr [5]. Such was not the case for NaCl [5] or KCl [6]. The interaction of H_2O with such active sites is expected either to stabilize water adsorbates up to room temperature or higher [1,4], or to cause dissociation [7]. All experimental techniques applied so far to alkali halides [2-7] were sensitive either to the composition or to the electronic structure of the adsorbate, but no measurements of the *geometrical* structure have been reported yet.

We are not aware of any work pertinent to water adsorption on alkaline-earth halides, in particular the fluorides, except for a report that the 2.8- μm -laser damage threshold of CaF_2 is correlated to the amount of adsorbed water [8]. The fluorite crystal structure suggests a different adsorption behavior for H_2O , compared to alkali halide substrates: On the (111) surface, the cation—which is the dominant adsorption site on alkali halides [4,9]—is partially buried by the top-layer fluorines, indicating a much shallower binding potential. On the other hand, we are intrigued by the fact that the ice-I structure is almost commensurate with that of $\text{BaF}_2(111)$, as indicated by the solid lines in Fig. 1: the F^- sublattice closely matches ice I [10,11]. Whether this influences water adsorption can only be tested either by microscopy with atomic resolution or by a technique which measures the adsorbate symmetry, such as second-harmonic generation (SHG) in reflection [12-14].

Although SHG is known to be very sensitive to adsorption of molecules on surfaces [14,15], it apparently has not yet been applied to the problem of water adsorption in UHV. In air, we have previously found a striking difference between the SHG azimuthal anisotropies of $\text{BaF}_2(111)$ and $\text{CaF}_2(111)$ [16]. In this Letter we report the first symmetry study of H_2O adsorption on these crystals by SHG under well controlled UHV conditions. Using single crystals of $\text{BaF}_2(111)$ and $\text{CaF}_2(111)$ with op-

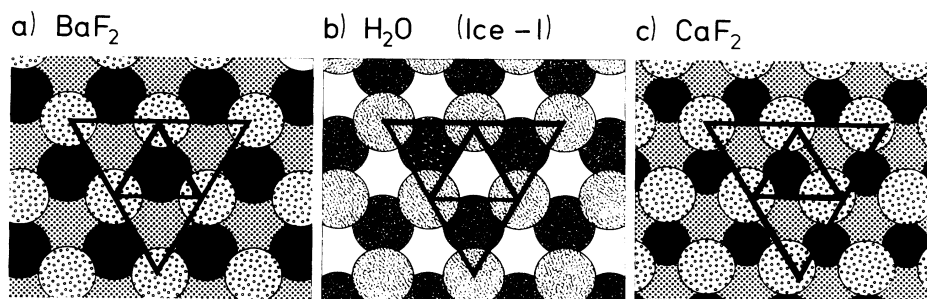


FIG. 1. Geometric structure of the (111) surface [10] for (a) BaF_2 and (c) CaF_2 and (b) of the face of hydrogen-bonded ice I [11]. In (a) and (c), the solid circles represent the metal ions and the dotted ones the fluorines. In (b), only the oxygens are shown. The O-H-O bond lengths of ice are indicated by solid lines.

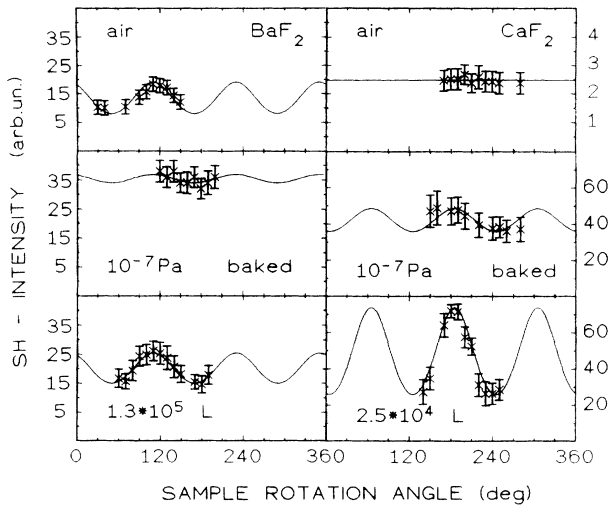


FIG. 2. Azimuthal dependence of SH yield from BaF₂(111) (left) and CaF₂(111) (right) in air, and from clean baked and water exposed surfaces (*p*-polarized fundamental and *p*-polarized second harmonic). The solid lines are least-squares fits by Eq. (1). For ease of operation, the fundamental intensity was higher for CaF₂ than for BaF₂. Consequently, the absolute SH intensities are not comparable for the two substrates. For technical reasons in the UHV chamber only part of the full 360° sample rotation could be performed. The angular dependence obtained from this interval agrees well with the previous result from a full rotation [16].

tically polished (111) surfaces [17] we find, in contrast to earlier observations on cleaved alkali halides [2-6], stable water adsorption even at room temperature, marked by a distinct azimuthal anisotropy.

The crystals were mounted in a UHV chamber with a base pressure of better than 10^{-9} Torr. Water vapor was leaked into the chamber at well-defined rates, exposing the surface to a controlled water dosage. The crystals were heated to about 700 K for at least 5 h, which reproducibly removed any adsorbed water. As fundamental light we used *p*-polarized laser radiation of 532 nm ($\tau = 6$ ns, $I \approx 10^7$ W/cm²), incident at 45° to the surface normal. The *p*-polarized second-harmonic (SH) yield was recorded as a function of angle between the plane of incidence and the azimuthal orientation of the surface.

In a control measurement, we reproduced our previous results [16] by exposing both samples for 1 day to laboratory air. For BaF₂(111) the 3*m* surface symmetry was obtained (see upper left of Fig. 2), whereas for CaF₂(111) only weak, azimuthally isotropic SHG emerged (upper right of Fig. 2). In UHV, we studied the azimuthal anisotropy as a function of water dosage at room temperature. Two different procedures were applied: (1) The crystals were cleaned by heating to 700 K each time before new water exposure, thus ensuring well controlled conditions. Typical results are presented in Fig. 2. (2) After cleaning the crystal the water dosage

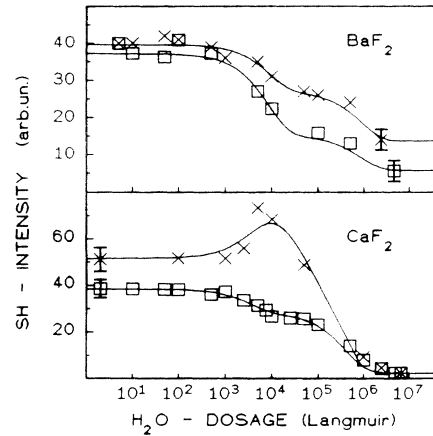


FIG. 3. Water dosage dependence of SH yield from BaF₂ (upper) and CaF₂ (lower) (111) surfaces. Shown is the maximum $(B+A)^2$ (\times) and minimum $(B-A)^2$ (\square) of the anisotropy [cf. Eq. (1)]. The solid lines are fits with the model of Langmuir kinetics, yielding the parameters of Table I.

was accumulated stepwise, measuring the maximum and minimum of the anisotropy at each step. This type of experiment enabled us to measure a large range of coverages in a reasonable time. The results are shown in Fig. 3.

The azimuthal dependence of the SH intensity $I_p(2\omega)$ for *p*-polarized fundamental and second-harmonic light can be written as [16]

$$I_p(2\omega) \propto I_p^2(\omega) |Af(\psi) + B|^2, \quad (1)$$

where $I_p(\omega)$ is the fundamental intensity. A and B represent the nonlinear polarizabilities parallel and perpendicular to the surface, respectively. $f(\psi)$ accounts for the surface symmetry in terms of the azimuthal angle ψ between the plane of incidence and a crystallographic reference direction. For the (111) orientation considered here $f(\psi) = \cos 3\psi$. Fitting the azimuthal dependences measured in the first type of experiments by Eq. (1), we obtained the ratios A/B for each dosage. In Fig. 4, these ratios A/B are plotted as a function of water dosage for BaF₂ and CaF₂. This result, together with the one from Fig. 3, yields information about the influence of water coverage on the nonlinear surface polarizabilities A and B . As a general tendency, we notice that the total SH yield decreases with coverage, reflecting a damping effect of the adsorbed water molecules on the total hyperpolarizability at the substrate surface. Second, there is a difference in the symmetry-related anisotropy between BaF₂ and CaF₂, the latter showing a maximum in anisotropy around 10^4 langmuirs (L) (1 L = 10^{-6} Torr sec), before a total decrease at higher dosages.

For a detailed analysis, we assume that the effect of water on the SHG depends linearly on the number of adsorbed molecules and hence on the coverage θ [14,15,18]. Accordingly, the amplitudes A and B may be modified by a coverage-correlated contribution:

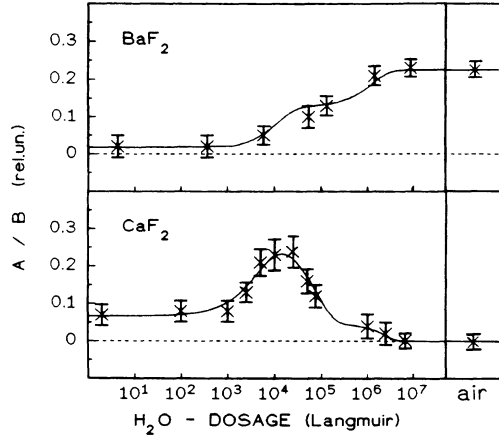


FIG. 4. Water dosage dependence of ratio A/B from BaF_2 (upper) and CaF_2 (lower) surfaces. The nonlinear polarizabilities parallel (A) and normal (B) to the surface are derived from the anisotropy data obtained by the experimental procedure (1) (cf. Fig. 2). The solid lines are fits with the model of Langmuir kinetics (parameters see Table I).

$$A = A_0 + A_1\theta/\theta_s, \quad B = B_0 + B_1\theta/\theta_s. \quad (2)$$

Here, θ_s represents a saturation coverage, index 0 denotes the pure substrate polarizability, and index 1 stands for the adsorbate-induced modification. In order to evaluate θ , one can take advantage of the previous observation [6] that water adsorption on salt crystals obeys Langmuir kinetics: Assuming that the sticking probability for each water molecule is independent of coverage as long as there exists equivalent adsorption conditions (sites or interaction potentials) and neglecting desorption, the water coverage depends on the applied dose D as [14,15,18]

$$\theta(D) = \theta_s (1 - \exp\{-\alpha D/\theta_s\}), \quad (3)$$

where the constant α is directly proportional to the sticking coefficient. A comparison of this model with experiment shows that one adsorption site is not sufficient to explain the data in Figs. 3 and 4. Agreement can be obtained by introducing several saturation values into Eq. (2), corresponding to different adsorption sites. The respective polarizabilities are then given by

$$A = A_0 \left(1 + \sum_i a_i (1 - \exp\{-D/S_i\}) \right) \quad (4)$$

and

$$B = B_0 \left(1 + \sum_i b_i (1 - \exp\{-D/S_i\}) \right), \quad (5)$$

with $a_i = A_i/A_0$, $b_i = B_i/B_0$, and $S_i = \theta_{s,i}/\alpha_i$.

The parameters for BaF_2 and CaF_2 , obtained by least-squares fits to the experimental data in Figs. 3 and 4, are listed in Table I and indicated in the figures by solid lines. Despite the two different experimental procedures, only one set of coefficients is required to fit both data sets. This is a justification for using the accumulative method

TABLE I. Saturation doses S_i ($\pm 10\%$) and relative nonlinear polarizabilities a_i, b_i (± 0.02). S_i given in units of langmuir ($1 \text{ L} = 10^{-6} \text{ Torrsec}$).

	BaF_2	CaF_2
S_1 (L)	1×10^4	5×10^3
S_2 (L)	...	6×10^4
S_3 (L)	1×10^6	1×10^6
a_1	8.5	3.43
a_2	...	-3.88
a_3	1.5	-0.55
b_1	-0.25	0.05
b_2	...	-0.26
b_3	-0.27	-0.64
A_0/B_0	0.02	0.07

and means that any water coverage is stabilized on the substrate, even at room temperature. The steps in Figs. 3 and 4 as well as the maximum for CaF_2 are well reproduced by assuming for BaF_2 two and for CaF_2 three different adsorption sites [17]. From the different signs of the a_i and b_i in Table I, it appears that adsorbed water can both amplify and attenuate the nonlinear polarizability of the substrate. The component oscillating normal to the surface (B) becomes, except for low coverage on CaF_2 , continuously weaker with increasing coverage, finally approaching the saturation value corresponding to air. This effect may be understood as a reduction of electron mobility normal to the surface. The A component, related to oscillations parallel to the surface, behaves differently: (i) At low doses, associated with S_1 , we find for both substrates a pronounced increase of the parallel hyperpolarizability, preserving the principal crystallographic directions of the substrate surface. (ii) For higher coverages, the effect of adsorbed water is different on $\text{BaF}_2(111)$ and $\text{CaF}_2(111)$. On BaF_2 , adsorption at the second type of sites preserves the $3m$ symmetry of the substrate up to air (cf. Fig. 2, left). In contrast, on CaF_2 the orientational effect decreases above $\approx 10^4 \text{ L}$ (Figs. 3 and 4). For still higher doses ($S_3 \approx 10^6 \text{ L}$), there appears a third type of adsorption site, where additional water molecules reduce the normal and parallel electron mobilities equally.

In order to understand the experimental results we note that the SHG technique measures the symmetry at the interface. We assume the adsorption to be nondissociative. This is supported by infrared absorption spectra of water on both substrates in air, showing a clear signature of the H_2O scissor vibration. Furthermore, the frequency-doubled radiation does not have sufficient photon energy (4.66 eV) to break the H-OH bond of 5.11 eV. Then, it appears reasonable to identify the first adsorption site (S_1) with a binding of the H_2O molecules to the substrate, with the dipoles partially oriented according to the surface symmetry. The particularly large enhancement of the SH yield on CaF_2 for this site suggests that here

the water dipoles are tilted almost parallel to the surface.

At the high dosage site (S_3), the water-water binding energy is stronger than the adsorption energy to the substrate, leading to formation of hydrogen-bonded bilayers, as is well known for metal surfaces of $3m$ symmetry [1]. As pointed out before, ice I is nearly commensurate with $\text{BaF}_2(111)$ [Figs. 1(a) and 1(b)], suggesting pseudomorphic epitaxial growth which preserves the substrate symmetry for all coverages, as observed experimentally. For CaF_2 , on the other hand, the crystal structure is not commensurate with ice I [Figs. 1(b) and 1(c)]. Consequently, before hydrogen bonds can form, a reorientation has to take place, which we believe is the intermediate phase of adsorption on CaF_2 (S_2). This reorientation leads to the observed destruction of the anisotropy.

In conclusion, we have for the first time applied SHG to obtain information about the interface symmetry for water adsorption on alkaline-earth halide surfaces. In agreement with previous results for alkali halides [6], we found that the adsorption dynamics can be well described by a simple Langmuir model. The total SH yield decreases, reaching a stable value above a dosage of 10^6 L. The coverage dependence of the azimuthal SHG anisotropy shows for both substrates at first an increase of the polarizability reflecting the substrate symmetry. This indicates oriented adsorption in the first step. For BaF_2 , this symmetry is preserved at higher coverages, whereas it is lost for CaF_2 . This points to epitaxial growth of water on $\text{BaF}_2(111)$ and a symmetry-destroying reorientation on $\text{CaF}_2(111)$. It remains an open question why molecular water readily forms stable adsorbates at room temperature on polished (111) surfaces of BaF_2 and CaF_2 , while for cleaved alkali halide surfaces low temperatures are required [5,7].

We thank Dave Beach of IBM, Yorktown Heights, for measuring the infrared absorption of our samples. Support by the Deutsche Forschungsgemeinschaft, Sonder-

forschungsbereich 337, is gratefully acknowledged.

-
- [1] P. A. Thiel and T. E. Madey, *Surf. Sci. Rep.* **7**, 211 (1987).
 - [2] R. A. Lad, *Surf. Sci.* **12**, 37 (1968).
 - [3] H. U. Walter, *Z. Phys. Chem.* **75**, 287 (1971).
 - [4] P. B. Barraclough and P. G. Hall, *Surf. Sci.* **46**, 393 (1974).
 - [5] J. Estel, H. Hoinkes, A. Kaarmann, H. Nahr, and H. Wilsch, *Surf. Sci.* **54**, 393 (1976).
 - [6] H. Kaarmann, H. Hoinkes, and H. Wilsch, *J. Chem. Phys.* **66**, 4572 (1977).
 - [7] S. Fölsch and S. Henzler, *Surf. Sci.* **247**, 269 (1991).
 - [8] S. D. Allen, J. O. Porteus, and W. N. Faith, *Appl. Phys. Lett.* **41**, 416 (1982).
 - [9] B. Wassermann, S. Mirbt, J. C. Zink, J. Reif, and E. Matthias (to be published).
 - [10] R. W. G. Wyckoff, *Crystal Structures* (Wiley, New York, 1963).
 - [11] D. Eisenberg and W. Kauzmann, *The Structure and Properties of Water* (Clarendon, Oxford, 1969).
 - [12] Y. R. Shen, *Annu. Rev. Mater. Sci.* **86**, 69 (1986).
 - [13] H. W. K. Tom, T. F. Heinz, and Y. R. Shen, *Phys. Rev. Lett.* **51**, 1983 (1983).
 - [14] G. L. Richmond, J. M. Robinson, and V. L. Shannon, *Prog. Surf. Sci.* **28**, 1 (1988).
 - [15] H. W. K. Tom, C. M. Mate, X. D. Zhu, J. E. Crowell, T. F. Heinz, G. A. Somorjai, and Y. R. Shen, *Phys. Rev. Lett.* **52**, 348 (1984).
 - [16] J. Reif, P. Tepper, E. Matthias, E. Westin, and A. Rosén, *Appl. Phys. B* **46**, 131 (1988).
 - [17] We also checked the response of cleaved surfaces and did not find any qualitative difference to polished samples, assuring that polishing does not cause artificial effects. Polished surfaces, however, guarantee well-defined reflection conditions, considerably facilitating the experiment.
 - [18] D. Heskett, L. E. Urbach, K. J. Song, E. W. Plummer, and H. L. Dai, *Surf. Sci.* **197**, 225 (1988).

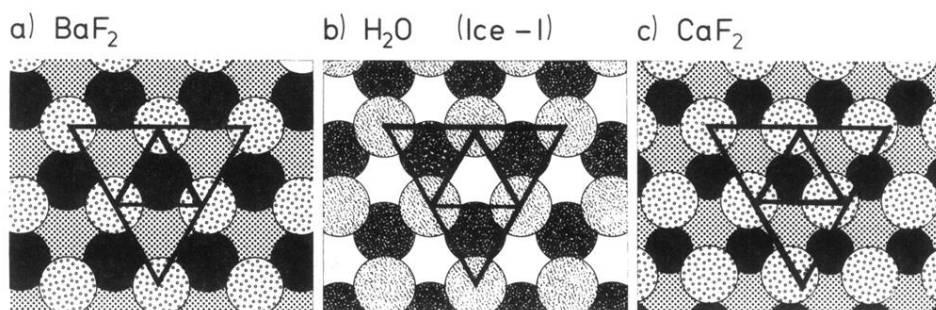


FIG. 1. Geometric structure of the (111) surface [10] for (a) BaF_2 and (c) CaF_2 and (b) of the face of hydrogen-bonded ice I [11]. In (a) and (c), the solid circles represent the metal ions and the dotted ones the fluorines. In (b), only the oxygens are shown. The O-H-O bond lengths of ice are indicated by solid lines.